

11th CIRP Conference on Photonic Technologies [LANE 2020] on September 7-10, 2020

Pre and post-treatments to improve weldability and mechanical properties of aluminum-polyamide laser welded specimens

Mahdi Amne Elahi^{a,*}, Marcus Koch^b, Mike Heck^a, Peter Plapper^a

^aUniversity of Luxembourg, 6, rue Coudenhove-Kalergi, L-1359, Luxembourg

^bINM – Leibniz Institute for New Materials Campus D2 2, 66123 Saarbrücken, Germany

* Corresponding author. Tel.: +352-466644-5885; fax: +352-466-644-35885. E-mail address: mahdi.amneelahi@uni.lu

Abstract

The laser polishing surface treatment is a prerequisite for enhanced weldability that is enabled by superior adhesion between the weldments. The paper describes the laser polishing process of the aluminum surface to develop a relatively thick and porous artificial aluminum oxide layer. Microscopic observation shows the laser polishing process significantly improves the adhesion of molten polyamide to the aluminum surface. Besides, the shear load of the pretreated joints is much higher than that of as-received ones. However, for the majority of the welded samples, the failure happens at the polyamide near the interface of aluminum/polyamide due to the thermal effect and structural changes of polyamide during the welding process. By applying the post-treatment of the welded specimens with different cycles, the mentioned failure mechanism is not observed anymore. Therefore, the mechanical properties of the joint will be improved and reach to the limits of the base materials.

© 2020 The Authors. Published by Elsevier B.V.

This is an open access article under the CC BY-NC-ND license (<http://creativecommons.org/licenses/by-nc-nd/4.0/>)

Peer-review under responsibility of the Bayerisches Laserzentrum GmbH

Keywords: laser welding of aluminum-polyamide; laser polishing; polyamide heat treatment; failure mechanism; artificial aluminum oxide

1. Introduction

The laser welding process is a promising technology to manufacture lightweight hybrid metal-polymer assemblies and miniaturize the joints. The accurate control over the welding energy of the laser beam is required to weld metals to polymers considering the significant difference of their melting points in general [1]. In the case of polyamide 6.6, the rapid degradation happens above 330°C while the melting point is 260°C, which is less than half of the melting temperature of aluminum. Therefore, polyamide 6.6 is a heat-sensitive material [2,3]. In addition, to achieve load-bearing and reliable joints, the implementation of surface pre-treatment is essential. Several publications have reported on different surface treatments and the positive effect of mechanical interlocking [4,5]. However, the industrial application of the laser welding for metal-polymer components is limited due to the low mechanical properties of the joints and the lack of detailed understanding of the joint and failure mechanisms. The unreliability of the

weld due to the degradation of the polymer and bubble formation near the interface of metal/polymer is also an issue to be addressed as the presence of the bubbles reduces the joint strength [6]. Nevertheless, some studies reported on the positive effect of the bubble formation to fill the roughness of the metal surface and promote the mechanical interlocking. In other words, high vapor pressure caused by a rapid expansion of bubbles pushes the molten polymer toward the metal surface. [7]

The authors introduced the laser polishing process as a pre-treatment to reduce the aluminum surface roughness while improving the adhesion between aluminum and polyamide [8]. In the presented study, the effect of the laser polishing process on the aluminum surface has been studied. Moreover, by comparing the mechanical properties, cross-sections and fracture surfaces of the samples welded with different parameters, the degradation of base materials at the weld zone and failure mechanisms have been investigated. Finally, to

improve the mechanical properties further, post heat treatment has been applied to the welded specimens.

2. Experimental Procedure

1050-H24 aluminum alloy (60×30×0.5mm) (simply will be addressed as Al in the text) and polyamide 6.6 (75×25×4mm) (simply will be addressed as PA) were used for this study. All samples were wiped with ethanol (≥ 99.8%) before further processing. Furthermore, to control the humidity content of PA samples before the welding process, they were conditioned based on ISO 1110. The laser-based conduction joining process was done in an overlap configuration. Both the laser welding and the laser polishing pretreatment were implemented with a continuous wave fiber laser (TruFiber 400) under the atmospheric environment. Temporal and spatial modulations of the laser beam have been used to tightly control the heat flow from Al to PA. While the spatial modulation is fixed (circular oscillation of the laser beam with 0.5mm amplitude, wobble frequency of 500Hz and wobble repetition of 0.225mm) [8], the temporal modulation in term of modulated power from 200 to 320W in the steps of 20W is studied, which is explained in equation 1 and figure 1.

$$P_{\text{mod}} = t_{\text{mod}} \cdot f_{\text{mod}} \cdot P_p \quad (1)$$

P_{mod} : Modulated power [W]

t_{mod} : Modulated time [s]

f_{mod} : Modulation frequency [Hz]

P_p : Peak power [W]

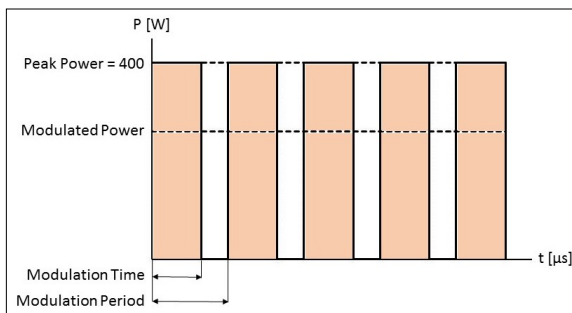


Fig 1. Power modulation of the laser beam.

For the welding process, the focal position of the laser beam is on top of the Al surface ($Z=0$) and the clamping force is constant for all samples. The surface roughness measurement of Al before and after the laser polishing process was done with a Mitutoyo SJ-500P based on ISO 4288-1996. The microscopic analysis of the Al surface was done with Transmission Electron Microscopy (TEM) (JEOL JEM-2100 LaB₆) after FIB (Focused Ion Beam) preparation (FEI Versa3D). Therefore, the as-received Al was covered with Platinum (Pt) before using a Gallium ion beam for TEM lamella preparation. For the laser polished surface, an additional amorphous carbon layer was deposited by evaporation before Pt coating. The cross-section was investigated by bright-field TEM imaging and diffraction. The cross-section of the welded specimen and the fracture surfaces were studied with Optical Microscopy (OM) (Leica

DM 4000 M and Keyence VHX-5000) and Scanning Electron Microscopy (SEM) (with FEI ESEM Quanta 400 FEG). The cross-sections have been prepared from the middle of the weld path in length. The heat treatment on the samples was done at 50, 100, 150 and 200°C for 3 hours (with a Memmert vacuum oven) and finally to evaluate the mechanical properties of the joints the tensile-shear test (Zwick/Roell machine) with the maximum force of 5KN and constant speed of 2.5mm/min was implemented. The reported values are the average of at least five independent measurements.

3. Results and Discussions

Figure 2 shows the FIB cut for Al surfaces and the corresponding TEM images. Al surface in as-received condition has a noticeable roughness orthogonal to the rolling direction (on average 0.62μm). Applying the laser polishing process significantly reduces the roughness (on average 0.18μm). However, due to surface melting under the atmospheric environment during the laser polishing process, a relatively thick porous layer of Al oxide is generated on the Al surface. The natural Al oxide that is found on the as-received Al sample is approximately 25nm thick and amorphous, as indicated by high-resolution TEM. However, the porous artificial Al oxide layer is approximately 1.5μm thick and crystalline. TEM diffraction of the Al oxide layer shows distinct spots in the image (data not shown).

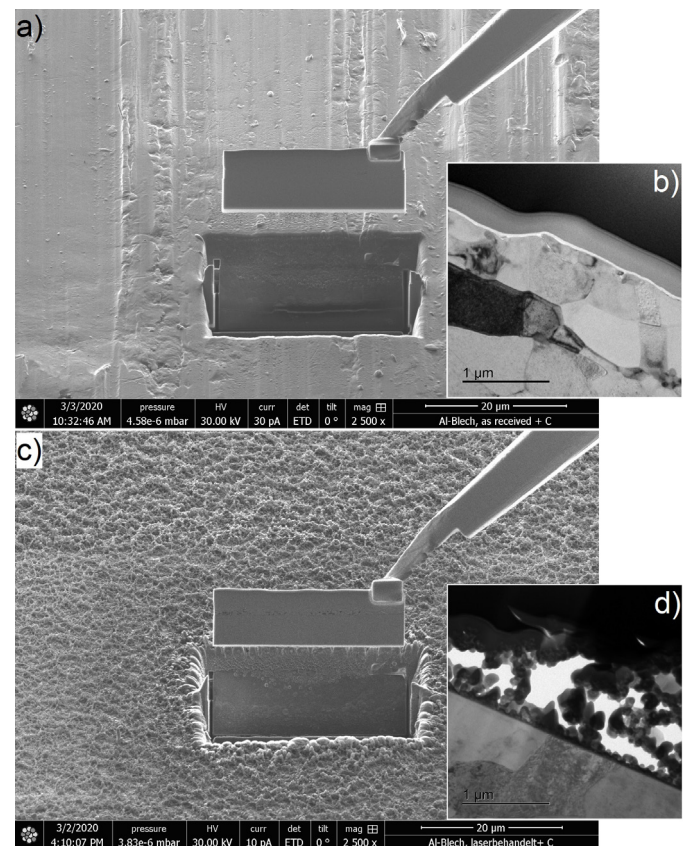


Fig. 2. a) FIB cut for as-received Al sample, b) TEM image of as-received Al, c) FIB cut for laser-polished Al, d) TEM image of laser polished Al.

Figure 3 shows the shear loads of the untreated and pretreated Al samples welded to PA and the corresponding failure during the test. By increasing the modulated energy for as-received and laser-polished Al, an improvement of the shear load is recorded until 300W. Afterward, both graphs follow reduction trends due to the thermal pyrolysis of PA.



Fig. 3. The shear load of the samples with the corresponding failure type.

Figure 4 depicts a comparison between the cross-sections of welded specimens with and without the PA thermal pyrolysis. Thermal pyrolysis of PA already starts at 300W modulated energy in the form of small distributed bubbles at the interface of Al/PA, however as the formation of bubbles is extreme at 320W, the failure of Al at the weld area and reduction of the tensile shear load can be recorded due to lower cross-section of Al.

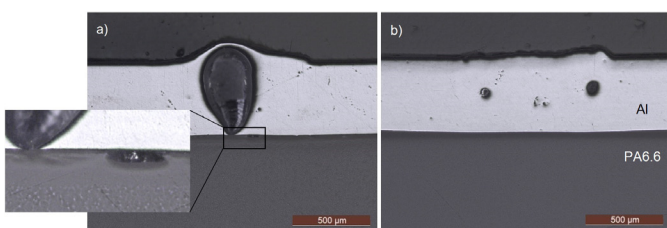


Fig. 4. a) The presence of bubbles due to thermal pyrolysis of PA, b) welding with optimum modulated energy to avoid PA thermal pyrolysis.

For each modulated energy, the pretreated Al surface provides a higher shear load for the welded specimens. There are three different types of failures during the test. The entire welded specimens with as-received Al fail at PA near the interface of Al/PA regardless of the welding energy (near adhesive failure). Pretreated samples welded with modulated energy lower than 240W also fails similarly. However, there is a major difference between the fracture surfaces of pretreated and untreated samples. Figure 5 shows the top views of PA fracture surfaces for different samples.

As can be observed for as-received Al welded with low modulated power, the failure is almost adhesive while by merely increasing the modulated energy, some droplets appear on the fracture surface of Al that is removed from PA. For pretreated samples welded with modulated energy up to 240W a continuous layer of PA breaks from PA and sticks to the Al surface. The thickness and width of this layer depend on the modulated energy.

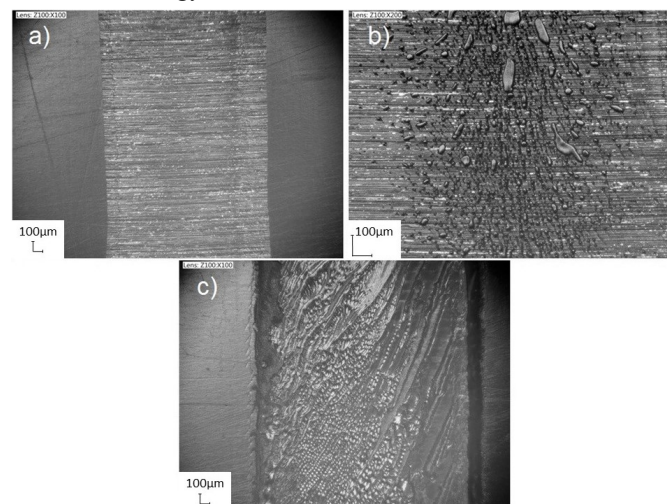


Fig. 5. PA fracture surfaces, a) untreated sample welded with 240W-modulated power, b) untreated sample welded with 260W, c) pretreated sample welded with 260W.

In other words, molten PA does not wet as-received Al surface uniformly thus represents low adhesion while applying the laser polishing on the Al surface, the adhesion improves significantly. Having in mind the presence of a natural Al oxide layer on top of as-received Al, this layer is dense and does not provide good wettability for molten PA. In contrast, the artificial Al oxide is quite porous and relatively thicker, therefore the molten PA can effectively infiltrate the artificial Al oxide. Taking into account the results of the tensile-shear test, the improvement of wettability results in the superior mechanical properties of the joint. By further increase of the modulated power of the welding process for the pretreated samples, the welded area between Al and PA gets bigger, therefore, thanks to the higher anchoring between Al and PA, the joint is stronger than the PA at the weld zone, therefore the PA fails during the test. Finally, with the escalation of PA degradation at high-modulated energies, Al fails at the weld zone due to bubble formation. The failure of PA or Al at the weld zone does not happen for as-received Al samples as the load-bearing connection between Al and PA at the surface is separated droplets, which are stress concentration points to be failed earlier than the other areas.

Figure 6 shows the welded cross-section schematic of a pretreated sample based on microscopic observation. As can be seen, because of the heat flow from the Al to PA surface in the laser welding process, a layer of PA melts and adheres to Al. The size of this layer (both size and depth) gradually increases with the elevation of the welding energy. Other researchers

reported the presence of such a layer in metal/polymer welding [9].

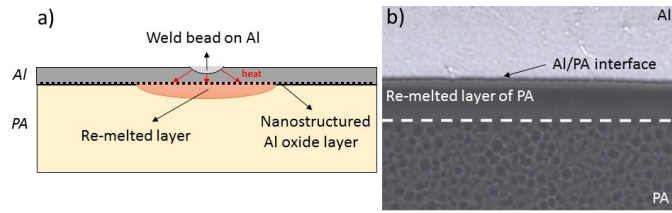


Fig. 6. a) Schematic of welded cross-section, b) microscopic observation of near Al/PA interface for a pretreated sample (not to scale).

Figure 7 depicts the measurement of the weld width for different samples, which is done with microscopic observation. In fact, for each modulated energy, the weld width of pretreated samples is higher than that of as-received ones. The lower surface roughness and therefore better heat flow between the weldments for pretreated samples, also better adhesion of the molten PA and artificial Al oxide is the reasons for the mentioned comparison.

Considering the figures 3 and 7, the improvement of the shear load for each category of untreated and pretreated samples until severe degradation of PA (320W-modulated energy) is because of the enlargement of the weld area. Therefore, the shear strength for each category is constant in case of near adhesive failure. For all untreated samples, the shear strength is 20 MPa on average; however, that of laser-polished samples with near adhesive failure (samples welded with up to 240W) is 23 MPa on average. For the other samples, the joint is stronger than the base materials at the weld zone.

As already discussed, the major type of failure during the mechanical test is near adhesive failure. In other words, a thin layer on PA breaks from the bulk and sticks to the Al surface. Doing 3D surface topography measurements on fracture surfaces and compare them to the cross-section observations of the welded specimens shows that the PA layer sticks to Al during the failure has good accordance with the re-melted layer, which has been introduced in figure 6. Therefore, the failure happened between the re-melted PA layer and the bulk in the Heat Affected Zone (HAZ).

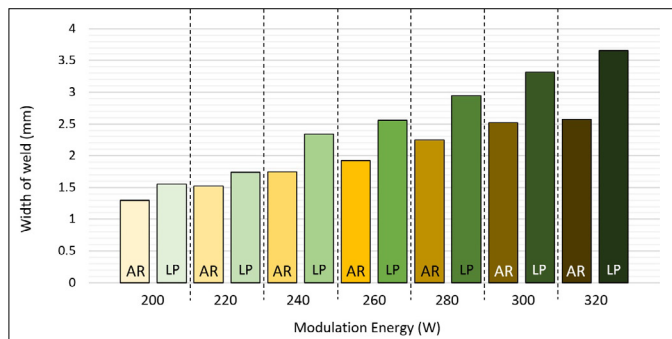


Fig. 7. Width of weld measurements for different samples. (AR: as-received, LP: laser-polished).

Figure 8 represents the comparison of microscopic observation and analysis of a fracture surface for the thickness. Having in mind the formation of the re-melted layer is due to the rapid heating and cooling of PA during the laser welding

process. Therefore, it is reasonable to believe that this layer has a different structure compared to the bulk PA. Consequently, the HAZ located between the re-melted layer and the bulk PA fails during mechanical testing. The difference of structures between the mentioned areas will be studied more in detail separately for the next publications. However, to prove this hypothesis indirectly, post heat treatment applied to the welded specimens to better homogenize the PA structure across the thickness or at least to reduce the residual stress generated due to the formation of the re-melted layer. The post-heat treatment implemented at 50, 100, 150, and 200°C for 3 hours.

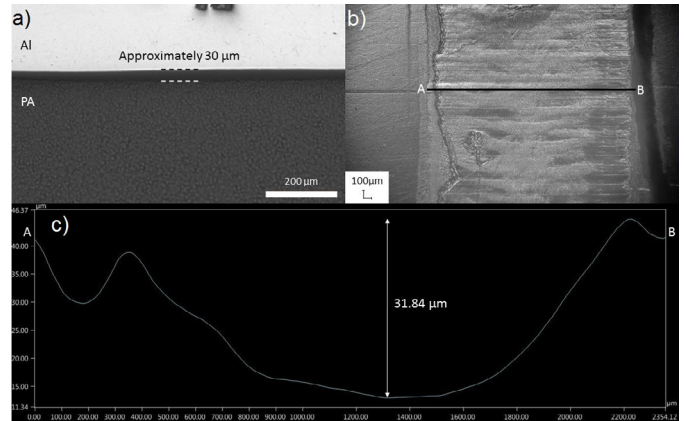


Fig. 8. a) The cross-section of laser-polished Al sample welded to PA with 260W modulated power, b and c) Measurements of the removed layer from PA fracture surface after the tensile-shear test for a similar sample.

Figure 9 shows the shear load after different cycles of heat treatment for untreated samples. All heat treatment cycles are detrimental to the mechanical properties of the joints in the untreated condition. In some cases, the joint already broke during the heat treatment process.

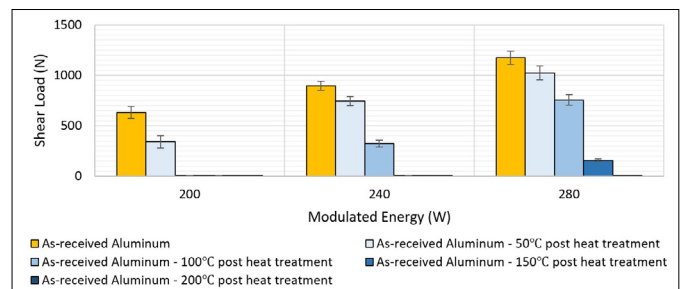


Fig. 9. Shear load of the as-received samples after the heat treatment.

There is a significant difference in thermal expansion between Al and PA (21-24 and 80 [10⁻⁶/K] respectively) [3,10]. Considering microscopic observations before and after the heat treatment process, as there is not a uniform connection between the weldments in untreated condition (the separated droplets, which is covered by weakly bonded and unbonded areas), thermal stress eliminates the weakly bonded areas then the separated droplets will break due to stress concentration. This makes the connection even weaker and at higher temperatures, the joint breaks eventually during the heat treatment process. Figure 10 shows a tilted view of an as-received Al fracture

surface. In contrast to untreated samples, the joint is quite continuous and uniform for the pretreated ones, which significantly reduces the stress concentration [8].

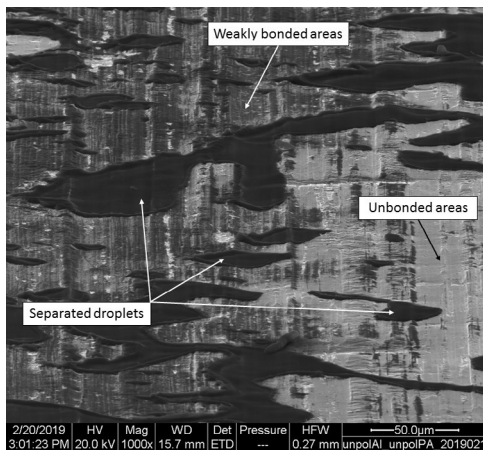


Fig. 10. Tilted view of an as-received Al fracture surface without the heat treatment process.

Figure 11 depicts the shear load of the pretreated Al welded to PA followed by the heat treatment process. Having continuous and uniform joint with the absence of stress concentration points, the positive effect of post heat treatment can be observed. However, getting near to the melting point of PA, at 200°C there is a significant drop in the mechanical properties of the joint due to the high thermal stress of PA. The deformation of PA samples in the oven is noticeable.

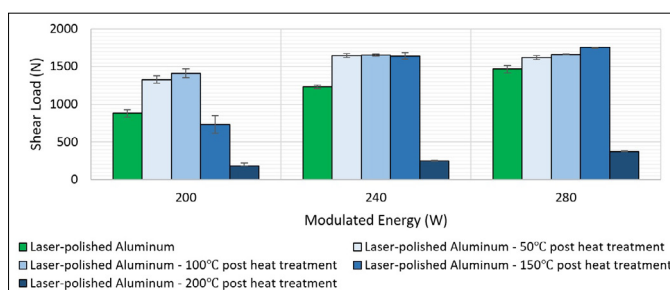


Fig. 11. Shear load of the pretreated samples after the heat treatment.

The reduction of the shear load also happens for the samples welded with 200W-modulated energy at 150°C as the weld between Al and PA has the minimum width. For other samples, there is a significant improvement in the shear load of the joints. For 240 and 280W samples heat-treated at 50, 100, and 150°C the joint is stronger than the base materials at the weld zone. Therefore, the tensile shear loads of the mentioned samples are comparable as the location of the failure is not the joint anymore. In other words, welding the samples with the medium modulation energy of 240W followed by post heat treatment can provide similar results to the corresponding samples of 280W, as the joint strength already passed the strength of the base materials. In conclusion, implementation of heat treatment on welded samples to reduce the residual

stress in HAZ, or make the PA structure more uniform, is only effective for pretreated samples, which are welded with appropriate welding energy.

4. Conclusion

- The laser polishing pretreatment of Al significantly improves the shear load of the joint thanks to the formation of a porous Al oxide layer, which is relatively thick and crystalline. This artificial layer provides excellent adhesion between molten PA and the surface of Al. In contrast, the natural Al oxide is relatively thin, dense, and amorphous.
- The shear load drops by increasing the modulated energy above the threshold of PA thermal pyrolysis due to the formation of bubbles at the interface of Al/PA.
- At the optimum modulated energy, the weld between Al and PA is stronger than the base materials at the weld zone.
- The re-melted PA layer and its HAZ during the welding process is responsible for near adhesive failure.
- The post-heat treatment process increases the shear load of the pretreated samples to the limits of the base materials.

Acknowledgments

The presented work is based on “Process Innovation for Sensors in Mobile Applications Based on Laser Assisted Metal-Plastic Joining” project (AFR-PPP grant, Reference 11633333). The authors would like to thank Birgit Heiland (INM) for excellent FIB sample preparation, the support of the Luxembourg National Research Fund (FNR), and acknowledge Cebi Luxembourg S.A. as the industrial partner

References

- [1] Lamberti C, Solchenbach T, Plapper P, Possart W. Laser assisted joining of hybrid polyamide-aluminum structures. *Phys Procedia* 2014; 56(C): 845-853.
- [2] Korshak VV, Slonimshii GL, Krongauz ES, *Isvest. Akad. Nauk. USSR. Otdel. Khim. Nauk* 1958; 221.
- [3] Technical datasheet of PA6.6, *dutec Kunststofftechnik GmbH*, www.dutec-kunststoff.de
- [4] Heckert A, Zaeh MF. Laser surface pre-treatment of aluminium for hybrid joints with glass fibre reinforced thermoplastics. *Phys Procedia* 2014; 56(C): 1171-81.
- [5] Heckert A, Singer C, Zaeh MF. Pulsed laser surface pre-treatment of aluminium to join aluminium-thermoplastic hybrid parts. *Lasers in Manufacturing (LiM) Conference* 2015.
- [6] Wang H, Chen Y, Guo Z, Guan Y. Porosity elimination in modified direct laser joining of Ti6Al4V and thermoplastics composites. *Appl Sci* 2019; 9(3).
- [7] Jung KW, Kawahito Y, Takahashi M, Katayama S. Laser direct joining of carbon fiber reinforced plastic to zinc-coated steel. *Mater Des* 2013; 47: 179-88.
- [8] Amne Elahi M, Koch M, Plapper P. Laser polishing of Aluminum and Polyamide for dissimilar laser welded assemblies. *Laser in Manufacturing (LiM) Conference* 2019.
- [9] Schrickler K, Bergmann JP. Temperature- and time-dependent penetration of surface structures in thermal joining of plastics to metals. *Key Engineering Materials* 2019; 809: 378-385.
- [10] https://www.engineeringtoolbox.com/linear-expansion-coefficients-d_95.html, date of access: 10/03/2020.